

## Valence State Transformation of Rh on CeO<sub>2</sub>NR/ $\gamma$ -Al<sub>2</sub>O<sub>3</sub> Composite Support

Yifan Wang<sup>1</sup>, Zhongqi Liu<sup>1</sup>, and Ruigang Wang<sup>1\*</sup>

<sup>1</sup>. Department of Metallurgical and Materials Engineering, The University of Alabama, Tuscaloosa, US.

\* Corresponding author: rwang@eng.ua.edu

Oxide supported catalysts are widely used in the heterogeneous catalysis industry nowadays. One of the most common industrial applications for oxide supported catalysts is in the automotive three-way catalytic converter (TWC). The reactions in TWC consist of CO oxidation, unburnt hydrocarbon oxidation and nitrogen oxides reduction. In the TWC application, CeO<sub>2</sub> is used as a support or promoter material to simultaneously promote two oxidation and one reduction reactions mentioned above, owing to the easy reversible valence state change between Ce<sup>3+</sup> and Ce<sup>4+</sup>.  $\gamma$ -Al<sub>2</sub>O<sub>3</sub> possesses high surface area with porous structure which promotes the dispersion of metal catalysts and reactant gas adsorption. In this study, ceria nanorods (CeO<sub>2</sub> NR), gamma alumina ( $\gamma$ -Al<sub>2</sub>O<sub>3</sub>) and their composites are chosen as the support materials for rhodium (Rh) catalyst to explore the origin of support prompting effect for low temperature CO oxidation.

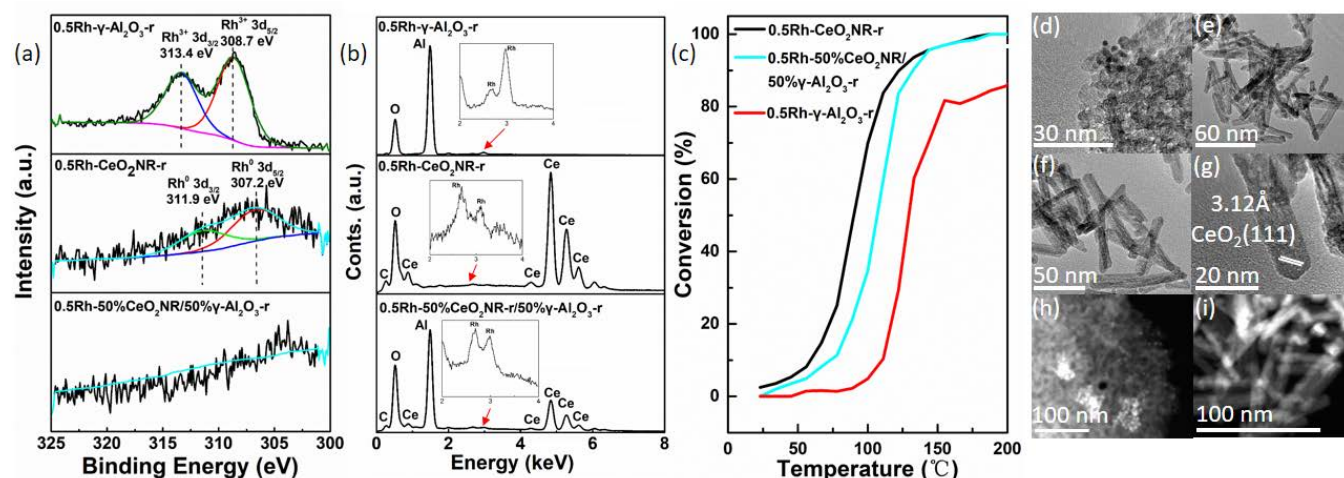
CeO<sub>2</sub> NR were synthesized by a hydrothermal method. Cerium nitrate hexahydrate (Ce(NO<sub>3</sub>)<sub>3</sub>·6H<sub>2</sub>O, 0.1 M) and sodium hydroxide (NaOH, 6M) were mixed in a 200 mL Teflon-lined autoclave and kept in a box furnace at 90 °C for 48 h. After the hydrothermal reaction, the sample was filtered and washed with 500 mL DI water and 50 mL ethanol. CeO<sub>2</sub> NR were obtained by drying the sample at 60 °C for 12 h.  $\gamma$ -Al<sub>2</sub>O<sub>3</sub> was synthesized by sol-gel method. Aluminum nitrate nonahydrate (Al(NO<sub>3</sub>)<sub>3</sub>) was first dissolved in DI water with urea and then the suspension was stirred for 1 h on a magnetic stirrer, filtered and dried. The dry powder was treated at 250 °C for 3 h and then heated at 500 °C for 3 h to obtain  $\gamma$ -Al<sub>2</sub>O<sub>3</sub> powder. The composites were obtained by mixing two supports (CeO<sub>2</sub> NR and  $\gamma$ -Al<sub>2</sub>O<sub>3</sub>) powders in solution with magnetic stirring. The catalysts with 0.5 wt.% Rh loading were prepared by direct wet-chemical deposition. An appropriate amount of rhodium chloride was dropwise added into the suspension solution of support powders and stirred for 24 h. Then sodium borohydride was added into the solution and stirred for 1 h. After filtering and drying, the catalyst powders were oxidized at 300 °C for 5 h in air and then reduced at 300 °C for 5 h under 5% H<sub>2</sub>/Ar flow. Finally, the catalysts were labelled as Rh-CeO<sub>2</sub>NR-r, Rh- $\gamma$ -Al<sub>2</sub>O<sub>3</sub>-r and Rh-50%CeO<sub>2</sub>NR/50% $\gamma$ -Al<sub>2</sub>O<sub>3</sub>-r (r refers to reduction treatment). The samples were characterized by XRD, BET surface area, Raman spectroscopy, XPS, and TEM. H<sub>2</sub> temperature programmed reduction (H<sub>2</sub>-TPR)/O<sub>2</sub> temperature programmed desorption (O<sub>2</sub>-TPD) were studied using a Micrometric AutoChem II 2920 chemisorption analyzer. The catalytic oxidation of CO was conducted using a fixed bed plug flow reactor system. The presence of CO and CO<sub>2</sub> were analyzed using an online gas chromatograph (SRI multiple gas analyzer GC, 8610C chassis).

Figure 1(a) shows the XPS spectra of Rh 3d for all three catalysts. A significant difference was observed in regard to the valence states of Rh among three catalysts: 0.5Rh- $\gamma$ -Al<sub>2</sub>O<sub>3</sub>-r only contains Rh<sup>3+</sup> species whereas 0.5Rh-CeO<sub>2</sub>NR-r contains Rh<sup>0</sup>, and no Rh was detected on the surface of 0.5Rh-50%CeO<sub>2</sub>NR/50% $\gamma$ -Al<sub>2</sub>O<sub>3</sub>-r. The different valence states were due to the respective support effect of CeO<sub>2</sub> NR and  $\gamma$ -Al<sub>2</sub>O<sub>3</sub> or Rh-support interaction. On  $\gamma$ -Al<sub>2</sub>O<sub>3</sub> support, it was reported that the existence of Rh<sup>3+</sup> is because Rh reacts with alumina irreversibly and forms an irreducible oxide phase [1]. On CeO<sub>2</sub> NR support, a strong interaction called oxygen ions back-spillover occurs between CeO<sub>2</sub> NR and RhO<sub>x</sub> at the interface [2]. It is not clear why there was little signal of Rh species for 0.5Rh-50%CeO<sub>2</sub>NR/50% $\gamma$ -

Al<sub>2</sub>O<sub>3</sub>-r. Two possible hypotheses are that, (a) due to the significant amount of surface defects on CeO<sub>2</sub> NR and strong CeO<sub>2</sub>- $\gamma$ -Al<sub>2</sub>O<sub>3</sub> interaction, Rh species diffuses in the lattice of the composite support; (b) Rh was encapsulated by porous layer of  $\gamma$ -Al<sub>2</sub>O<sub>3</sub> or reacted with  $\gamma$ -Al<sub>2</sub>O<sub>3</sub> to form rhodium aluminate (Rh(AlO<sub>x</sub>)<sub>y</sub>). The existence of Rh in all three samples was confirmed by the EDX analysis shown in Figure 1(b). The distribution of Rh species on these supports was characterized by TEM and STEM. Figure 1(d~g) show the TEM images of 0.5Rh- $\gamma$ -Al<sub>2</sub>O<sub>3</sub>-r (d), 0.5Rh-CeO<sub>2</sub>NR-r (e and g) and 0.5Rh-CeO<sub>2</sub>NR/ $\gamma$ -Al<sub>2</sub>O<sub>3</sub>-r (f), respectively. The STEM-HAADF images were shown in Figure 1(h) and (i) corresponding to the 0.5Rh- $\gamma$ -Al<sub>2</sub>O<sub>3</sub>-r and 0.5Rh-50%CeO<sub>2</sub>NR/50% $\gamma$ -Al<sub>2</sub>O<sub>3</sub>-r catalysts, respectively. Small RhO<sub>x</sub> nanoclusters can be observed only in 0.5Rh- $\gamma$ -Al<sub>2</sub>O<sub>3</sub>-r (h). No apparent RhO<sub>x</sub> clusters are found in 0.5Rh-50%CeO<sub>2</sub>NR/50% $\gamma$ -Al<sub>2</sub>O<sub>3</sub>-r (i) which is consistent with the XPS results (Figure 1(a)). Figure 1(b) shows the CO conversion of three catalysts. The brighter contrast clusters in Figure 1(h) represent the RhO<sub>x</sub> on  $\gamma$ -Al<sub>2</sub>O<sub>3</sub> surface due to Z-contrast. For the CO oxidation performance, shown in Figure 1(c), it is clear that 0.5Rh-CeO<sub>2</sub>NR-r shows the best low-temperature performance (below 120 °C) while 0.5Rh-50%CeO<sub>2</sub>NR/50% $\gamma$ -Al<sub>2</sub>O<sub>3</sub>-r has a similar catalytic activity as 0.5Rh-CeO<sub>2</sub>NR-r at higher temperature range (above 120 °C). Metallic Rh has been considered as the active site for CO oxidation in comparison with RhO<sub>x</sub> [3]. As a result of the strong CeO<sub>2</sub> NR-  $\gamma$ -Al<sub>2</sub>O<sub>3</sub> interaction, the diffusion and/or transformation of RhO<sub>x</sub> to other Rh species was promoted leading to the improved catalytic activity [4]. We will present more detailed interfacial structure and composition analysis.

#### References:

- [1] Suhonen, S. et al., *Appl. Catal. A Gen.* **218** (2001), p. 151.
- [2] Vayenas, C.G. et al., *Chem. Mater.* **16** (2004), p. 2317.
- [3] Gustafson, J. et al., *ACS. Catal.* **8** (2018), p. 4438.
- [4] The authors acknowledge funding from National Science Foundation (CHE-1657943) and American Chemical Society Petroleum Research Fund (#52323).



**Figure 1.** (a) XPS spectra, (b) EDX results, (c) CO conversion, TEM images of (d) 0.5Rh- $\gamma$ -Al<sub>2</sub>O<sub>3</sub>-r, (e, g) 0.5Rh-CeO<sub>2</sub>NR-r, (f) 0.5Rh-50%CeO<sub>2</sub>NR/50% $\gamma$ -Al<sub>2</sub>O<sub>3</sub>-r, and Z-contrast images of (h) 0.5Rh- $\gamma$ -Al<sub>2</sub>O<sub>3</sub>-r and (i) 0.5Rh-50%CeO<sub>2</sub>NR/50% $\gamma$ -Al<sub>2</sub>O<sub>3</sub>-r.